



Isotope ratios of precipitation and water vapor observed in Typhoon Shanshan

H. Fudeyasu,¹ K. Ichianagi,¹ A. Sugimoto,² K. Yoshimura,³ A. Ueta,² M. D. Yamanaka,¹ and K. Ozawa⁴

Received 23 August 2007; revised 22 January 2008; accepted 14 February 2008; published 26 June 2008.

[1] Isotope ratios of precipitation and water vapor were observed during the passage of Typhoon Shanshan at Ishigaki Island, southwestern Japan, on 15–16 September 2006. Such high-resolution isotopic observations allow for qualitative understanding of atmospheric moisture cycling; they revealed that isotope ratios of both the precipitation and water vapor decreased radially inward in the cyclone's outer region; anomalously high isotope ratios appeared in the cyclone's inner region; and d-excess tended to decrease in the cyclone's inner region. In the cyclone's outer region, the water vapor was isotopically depleted due to the rainout effect which involves both condensation efficiency as reflected in inwardly increasing cloud thickness and isotopic exchange between falling droplets and the ambient water vapor. In contrast, water vapor in the cyclone's inner region was isotopically enriched due to weak rainout effect in conjunction with intensive isotopic recharge from the sea spray and sea surface with heavy isotope ratios. Since water vapor mainly acts as a source of precipitation, the isotope ratios of precipitation also had systematic variation. A unique circumstance is the intensity of isotopic exchange with almost saturated surface air and high winds, causing anomalously high isotope ratios and low d-excess values in the cyclone's inner region.

Citation: Fudeyasu, H., K. Ichianagi, A. Sugimoto, K. Yoshimura, A. Ueta, M. D. Yamanaka, and K. Ozawa (2008), Isotope ratios of precipitation and water vapor observed in Typhoon Shanshan, *J. Geophys. Res.*, *113*, D12113, doi:10.1029/2007JD009313.

1. Introduction

[2] A number of studies have examined intensification of tropical cyclones (TCs) over the ocean [e.g., *Ooyama*, 1964, 1969; *Charney and Eliassen*, 1964; *Rotunno and Emanuel*, 1987; *Emanuel*, 1989; *Montgomery et al.*, 2006]. The main energy source of a TC is the water derived from evaporation from a tropical ocean and/or converging water vapor in the atmospheric boundary layer from environmental moisture surrounding the TC. While atmospheric moisture cycling plays a central role in TC intensification, few observations of such moisture cycling are available. Stable hydrogen and oxygen isotope ratios ($^2\text{H}^1\text{H}^{16}\text{O}/^1\text{H}_2^{16}\text{O}$ and $^1\text{H}_2^{18}\text{O}/^1\text{H}_2^{16}\text{O}$) are dynamic tracers of atmospheric moisture cycling because their compositions are physically influenced by complex atmospheric behavior, water vapor advection, condensation, and evaporation. Many observational studies have examined isotopes of precipitation and water vapor [e.g., *Ichianagi et al.*, 2005].

[3] *Lawrence and Gedzelman* [1996] suggested the use of stable isotope ratios to investigate the moisture cycling of TCs. The mean precipitation isotopes in TCs are markedly lower than those in other tropical and summer precipitation [*Lawrence*, 1998; *Lawrence and Gedzelman*, 2003; *Lawrence et al.*, 1998, 2004]. *Lawrence et al.* [1998] speculated that the low precipitation isotope ratios in TCs result from their high, thick clouds, large precipitation region, and relative longevity. Because of continuing fractionation during condensation, the isotope ratios of water vapor decrease as saturated air rises [*Gedzelman and Lawrence*, 1982], an example of the rainout effect [e.g., *Dansgaard*, 1964]. They also tend to be lower under thicker clouds, increases in the precipitation efficiency [*Lawrence and Gedzelman*, 1996], and downwind from a precipitation region.

[4] At the surface over land, studies have found that the isotope ratios of both the precipitation and water vapor in TCs decreased radially inward toward the eye [*Lawrence and Gedzelman*, 1996; *Lawrence et al.*, 1998, 2002]. The following two factors likely explain these decreases: the inward increase of precipitation efficiency due to higher cloud tops, and diffusive isotopic exchange between falling droplets and the ambient water vapor. Because lighter isotopes preferentially diffuse from condensates, the isotope ratios of droplets become heavier as they fall. In contrast, ambient water vapor is isotopically depleted in the heavier isotopes, one of the rainout effects. Therefore the precipitation condensed from this water vapor with lighter isotope ratios becomes isotopically lighter [*Miyake et al.*, 1968].

¹Japan Agency for Marine-Earth Science and Technology, Institute of Observational Research for Global Change, Yokosuka, Kanagawa, Japan.

²Hokkaido University, Graduate School of Environmental Science, Sapporo, Hokkaido, Japan.

³University of Tokyo, Institute of Industrial Science, Tokyo, Tokyo, Japan.

⁴Japan International Research Center for Agricultural Sciences, Tropical Agriculture Research Front, Ishigaki, Okinawa, Japan.

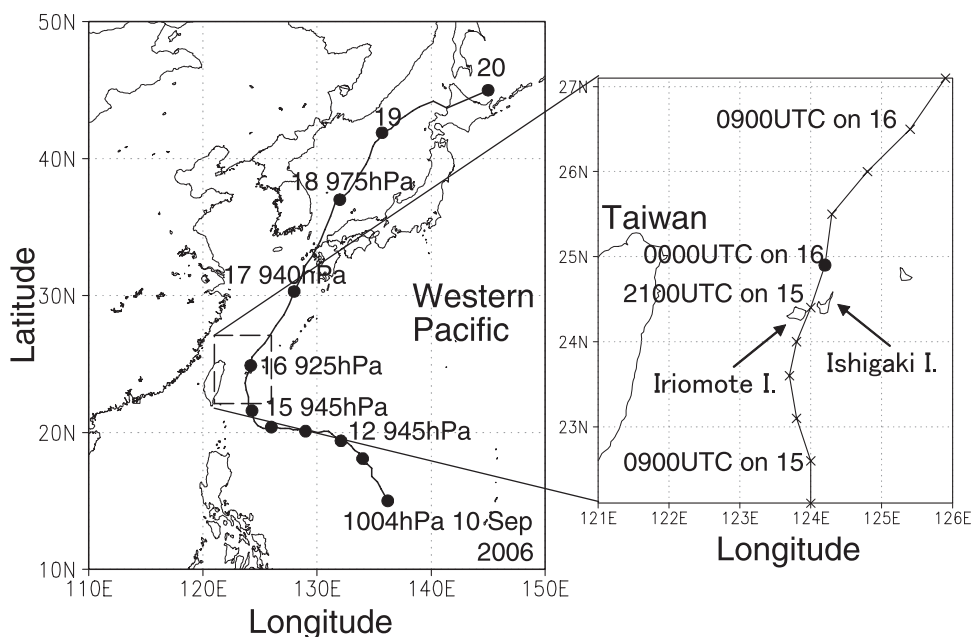


Figure 1. Track of Shanshan from Best Track data for the period 10–20 September 2006. Filled circles represent positions of Shanshan at 0000 UTC, while crosses represent positions at 0300, 0600, 0900, 1200, 1500, 1800, and 2100 UTC on 15 and 16 September 2006.

Lawrence *et al.* [1998] showed that a two-dimensional microphysical model with isotopic physical algorithms developed by Gedzelman and Arnold [1994] simulated idealized TC situations. The model calculated the inward decreases in isotope ratios of precipitation and water vapor caused by stepwise isotope exchange between falling precipitation and converging water vapor. Recently, Lawrence *et al.* [2006] reported the isotopic observation at the southern coast of US, finding the slightly higher isotope ratios of water vapor around the eye of Hurricane Katrina, 2005.

[5] In contrast to surface-based observational results, isotope ratios of precipitation and water vapor collected over the ocean at heights from 600 to 3000 m during flights in Hurricane Faith, 1967, quickly increased to high values in the eyewall [Ehhalt and Ostlund, 1970]. Gedzelman *et al.* [2003] collected precipitation and water vapor during flights into four hurricanes at flight levels between 850 and 475 hPa and analyzed the stable isotopes. The lowest isotope ratios occurred in or near regions of stratiform precipitation between about 50 and 250 km from the hurricane center, but isotope ratios increased inward in the eyewall. The occurrence of high isotope ratios in the eyewall suggests that a large fraction of the water vapor originates or is altered deep within the hurricane, where air just above the sea surface is filled with sea spray with heavy isotope ratios [Black *et al.*, 1986]. The results of a two-layer fractionation chamber model [Gedzelman *et al.*, 2003] showed that sea spray that filled the atmosphere [Wang *et al.*, 2001] supplied the eyewall with up to 50% of its water vapor and was largely responsible for its high isotope ratios.

[6] Although previous isotopic observations have provided much information, there is no isotopic “ground truth” that shows the isotope ratios and d-excess of water vapor in a TC eye during the intensification of a TC over the sea, accompanied by a sudden cessation of precipitation. This

may reflect either the coarse temporal interval of the operational observations or the difficulty in capturing a TC developing over subtropical seas, or both. We therefore attempted intensive surface-based observations with high temporal resolution of isotopes of both precipitation and water vapor in a TC passing over Ishigaki Island, Japan, during the passage of Typhoon Shanshan in mid-September 2006. We also made comprehensive meteorological observations so that we could analyze the features of the precipitation pattern accompanying Shanshan and better understand atmosphere moisture cycling in a TC developing over the sea. Moreover, it is noteworthy that this is the first report to describe surface-based measurement of isotope ratios and d-excess of water vapor in a TC eye over an island small enough to have little effect on the storm.

2. Data and Methods

2.1. Isotopic Data

[7] Intensive isotopic observations were conducted from 11 to 18 September 2006 at the Japan International Research Center for Agricultural Sciences (JIRCAS) on Ishigaki Island in southwestern Japan (Figure 1). Ishigaki Island is a small subtropical island that is 221 km² in area and is a convenient location to capture a TC developing over the subtropical sea.

[8] Precipitation samples were automatically collected for every 1-mm amounts of precipitation with an auto-precipitation sampler. Water vapor was cryogenically collected at liquid nitrogen temperature (−196°C) using an extraction line composed of a U-shaped glass tube filled with glass beads [Sugimoto *et al.*, 2002]. Air was introduced from an air inlet on the roof of the building into the extraction line in the laboratory of the JIRCAS through a polyethylene tube using a vacuum pump positioned at the outlet of the extraction line. The air intake for the water vapor sampling

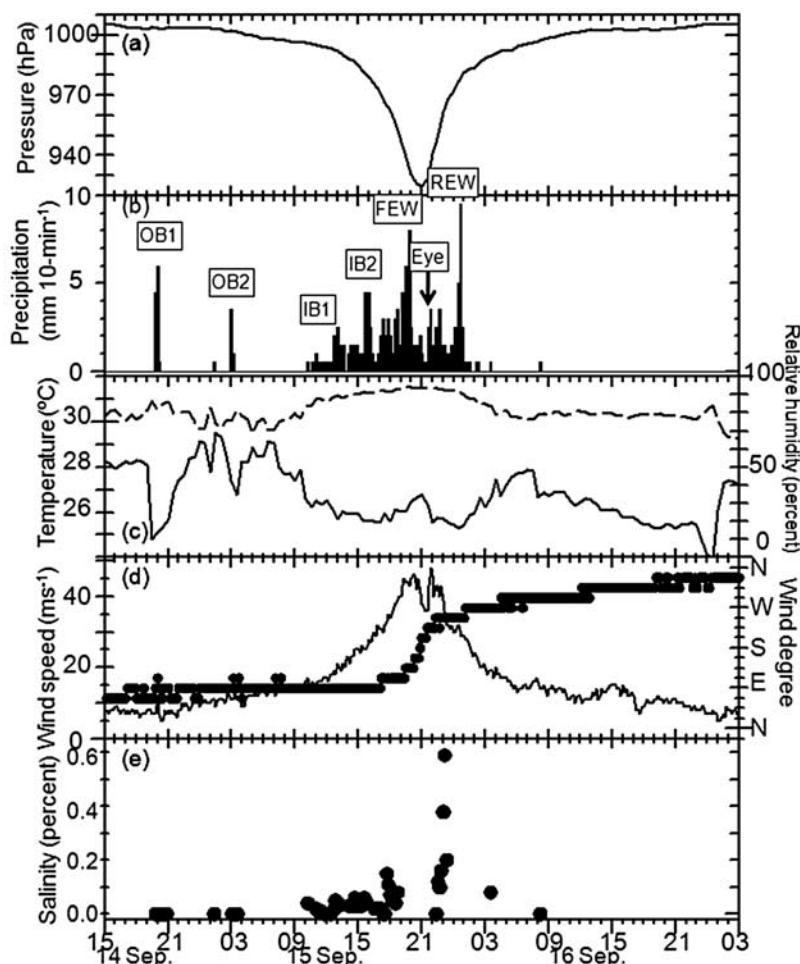


Figure 2. Record of (a) 30-min averaged surface pressure, (b) 10-min accumulated precipitation, (c) 30-min averaged temperature (solid line) and relative humidity (broken line), (d) 10-min averaged wind speed (line) and direction (dots), and (e) salinity in precipitation samples collected at Ishigaki Island from 1500 UTC on 14 September to 0300 UTC on 17 September 2006.

was adequately shielded from the precipitation. The flow rate of the air was reduced to about 300 mL min^{-1} for complete extraction of the water vapor. Sampling was continued until at least 0.3 mL of water was obtained; in other words, sampling duration depended on the mixing ratio of the air sample, and was generally about 70 min in our observations. At the end of sampling, carbon dioxide that was trapped with the water vapor was vaporized and removed by pumping out at liquid nitrogen ethanol slush temperature (-90°C). Water vapor samples were collected around 0430, 1030, 1630, and 2230 UTC every day.

[9] The isotopic composition of water samples was analyzed by the $\text{CO}_2/\text{H}_2/\text{H}_2\text{O}$ equilibration method using a mass spectrometer at the Graduate School of Environmental Science, Hokkaido University. Isotopic compositions are expressed with values defined as $\delta_{\text{sample}} = (R_{\text{sample}}/R_{\text{SMOW}} - 1) \times 1000$, where R_{sample} is the isotope ratio in the sample, and R_{SMOW} is the isotope ratio in the standard (i.e., standard mean ocean water, SMOW). The $\delta^2\text{H}$ and $\delta^{18}\text{O}$ values of water vapor and precipitation near sea level range from about +40 to -400 per mil and +5 to -50 per mil, respectively [Dansgaard, 1964]. Analytical errors were less than 2 per mil for $\delta^2\text{H}$ and 0.15 per mil for $\delta^{18}\text{O}$, respectively. Deuterium excess (d-excess) was calculated as

$d\text{-excess} = \delta^2\text{H} - 8 \times \delta^{18}\text{O}$. The magnitude of d-excess depends on several nonequilibrium processes [e.g., Craig, 1961; Merlivat and Jouzel, 1979]. The global average value measured in precipitation is 10 per mil.

[10] We also measured the salinity of the collected precipitation by a compact electric conductivity meter to detect the sea-spray content of the precipitation samples. Sea spray, which has heavy isotope ratios, like ocean water does, was trapped together with the falling droplet, causing an overestimate of precipitation isotope ratios. We therefore corrected the precipitation isotope ratios for sea spray content, roughly assuming that the isotope content of sea spray is 0 per mil as in ocean water. The correction equation is written as $\delta_{\text{correct}} = \delta_{\text{obs}}/(1 - S_{\text{obs}}/S_{\text{sea}})$, where δ_{correct} is the corrected isotope content of the sample, δ_{obs} is the isotope content of the observed sample, S_{obs} is the salinity of the observed sample, and S_{sea} is the 3.4% salinity of ocean water. This equation to correct for precipitation isotope ratios assumes that the salt derived from sea spray drops without evaporation. The average amount of salinity detected in precipitation samples was about 0.05% (Figure 2e). The largest amount of salinity, about 0.6%, was detected in precipitation around the TC center, causing about 1.0 per mil overestimation for $\delta^{18}\text{O}$. The isotope

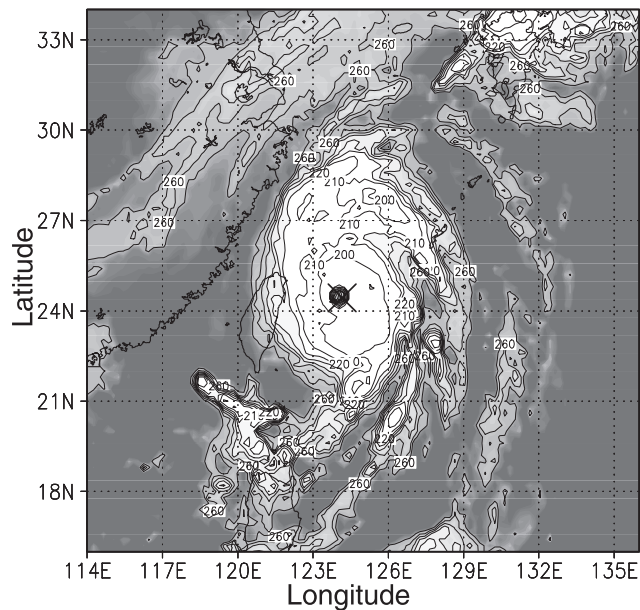


Figure 3. Equivalent blackbody temperature (T_{BB}) at 2100 UTC on 15 September 2006. The contour interval is 10 K. The cross marks the position of Ishigaki Island.

content of water vapor was not corrected because of the absence of sea spray in the water vapor samples.

2.2. Meteorological Data

[11] As meteorological data, we observed 1-min accumulated precipitation and 30-min averaged surface pressure, surface wind, temperature, and relative humidity at JIR-CAS. Surface wind data averaged over 10-min intervals derived from the Automated Meteorological Data Acquisition System (AMeDAS) of the Japan Meteorological Agency (JMA) at Ishigaki were also used. The precipitation pattern over Ishigaki Island was estimated from an operational weather radar map at Ishigaki site provided by the JMA. The radar echo data have a horizontal resolution of 1.0 km. The precipitation pattern was derived from the 2A12 product of the Tropical Rainfall Measuring Mission Microwave Imager (TRMM-TMI). The 2A12 data consist of instantaneous TRMM-TMI precipitation retrievals with a horizontal resolution of about 5.1 km. Equivalent blackbody temperatures (T_{BB}) taken from satellite images collected by the Geostationary Meteorological Satellite (MTSAT) were also used in this study. These satellite data have a horizontal resolution of 0.2° for both longitude and latitude.

[12] The track of Shanshan was obtained from the Best Track data of the Regional Specialized Meteorological Centers (RSMC) Tokyo-Typhoon Center. The data set consists of the names, positions, maximum surface pressure, and maximum wind speeds of TCs, recorded at 3-h intervals around Ishigaki Island. Estimates of the 10-min positions of the cyclone center were determined by spline interpolation of the 3-h data.

3. Results

3.1. Precipitation Pattern of Typhoon Shanshan

[13] Figure 1 shows the track of Typhoon Shanshan derived from the Best Track data. Shanshan was upgraded

from a tropical depression to a tropical storm (maximum 10-min sustained wind speed in excess of 17.2 m s^{-1}) at 1200 UTC on 10 September 2006, when situated at 16.8°N , 134.8°E . Shanshan moved westward and turned toward the north over the sea south of the Ishigaki Island on 14 September. Shanshan gradually increased in intensity over the warm sea and passed between Iriomote and Ishigaki islands at 2100 UTC on 15 September, with a central pressure of 925 hPa and a maximum wind speed in excess of 50 m s^{-1} . During the passage over Ishigaki Island, an eye approximately 30-km in radius became clearly visible in the satellite image (Figure 3). At that time, Ishigaki Island was located in the eye.

[14] Figure 2 shows a time series of surface observations at Ishigaki Island, while Figure 4 presents a radar map derived from the weather radar at the Ishigaki site. When Shanshan was located over the sea about 300 km south of Ishigaki Island, two outer rainbands (referred to as OB1 and OB2) quickly passed over Ishigaki Island at 1920 UTC on 14 September (Figure 4a) and 0320 UTC on 15 September (Figure 4b), causing heavy precipitation (Figure 2b). The precipitation accompanying these outer rainbands was characterized by heavy convective precipitation with subsequent stratiform precipitation.

[15] After 0900 UTC on 15 September, as Shanshan approached close to Ishigaki Island, easterly wind speed gradually increased, and relative humidity remained high at more than 90% (Figure 2c). The broad echo region spreading about 150 km from the eye, known as the rain shield [Shimazu, 1998], covered Ishigaki Island (Figure 4c), causing stratiform precipitation (Figure 2b). In the rain shield, two inner rainbands (referred to as IB1 and IB2) passed over Ishigaki Island (Figures 4d and 4e), causing heavy convective precipitation around 1300 and 1600 UTC on 15 September (Figure 2b). After IB2 had left, a ring of intense convection surrounding the center, front eye wall (referred to as the FEW), began to cover Ishigaki Island at 1800 UTC.

[16] Although a power failure due to the storm interrupted the weather radar observation after 1900 UTC on 15 September (Figure 4f), precipitation patterns associated with Shanshan were provided by TRMM-TMI observations at 0440 UTC on 16 September (Figure 5). During the passage of the FEW over Ishigaki Island from 1800–2040 UTC on 15 September, heavy convective precipitation and strong easterlies exceeding 45 m s^{-1} were observed at Ishigaki Island (Figures 2b and 2d). At 2040–2130 UTC, when Ishigaki Island was located in the weak echo region of the eye (Figure 5), there was a rapid shift to no or little precipitation and wind speed weakened with veering. The veering indicated that Ishigaki Island was to the right of the direction of Shanshan's movement. The lowest surface pressure of 924 hPa was recorded at this time (Figure 2a), while surface temperature increased (Figure 2c).

[17] Strong westerlies reached about 50 m s^{-1} following the passing of the eye (Figure 2d). The rear eye wall (referred to as the REW) brought the heaviest precipitation, in excess of 10 mm in 10 min. After the passage of the REW, the precipitation accompanying the rain shield ended over Ishigaki Island by 0200 UTC on 16 September. The wind speeds gradually decreased in association with the departure of Shanshan. As Shanshan moved away from

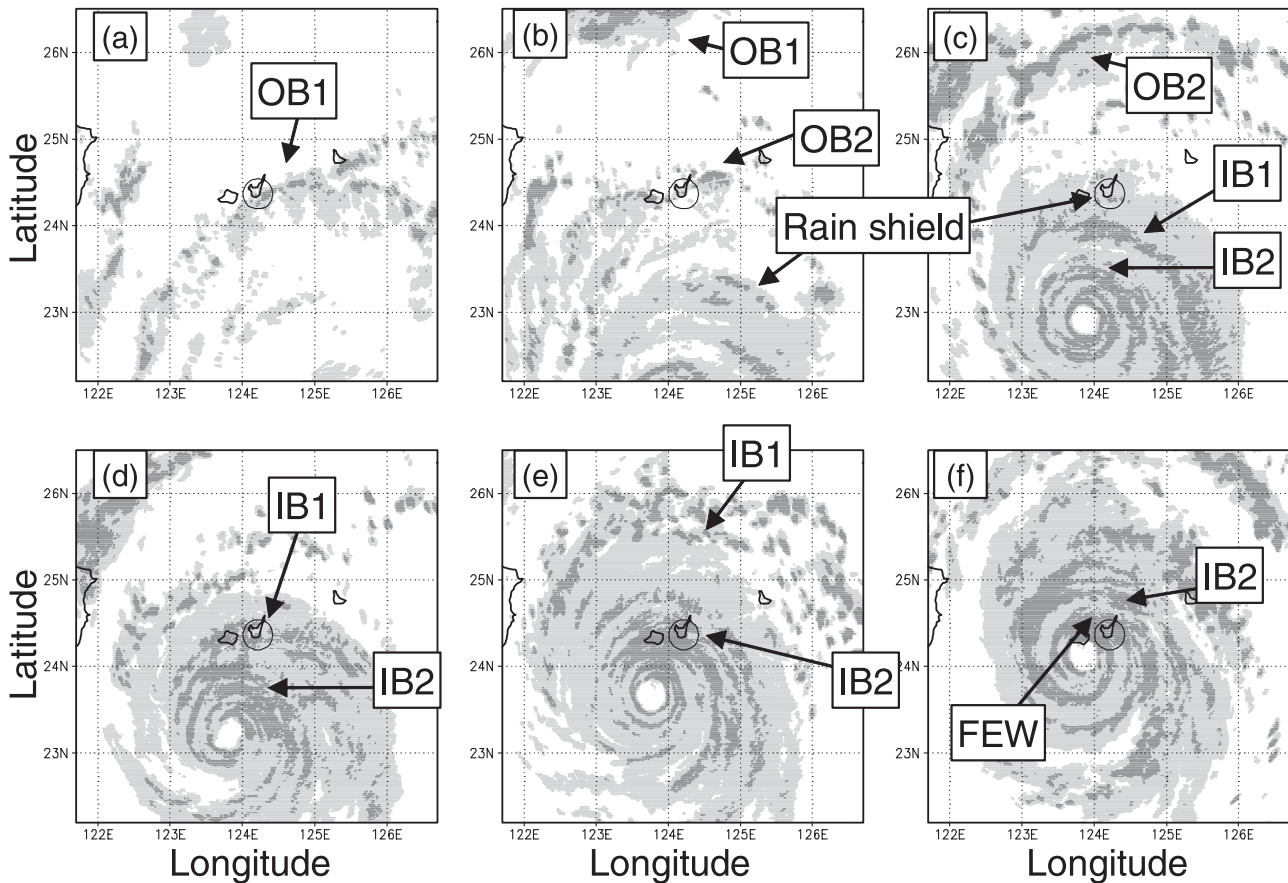


Figure 4. Radar map of the Ishigaki site at (a) 1920 UTC on 14, (b) 0320 UTC, (c) 1100 UTC, (d) 1300 UTC, (e) 1600 UTC, and (f) 1900 UTC on 15 September 2006. Light shading shows regions of echo intensity of 10–40 mm h⁻¹, while darker shading indicates regions of echo intensity greater than 40 mm h⁻¹. Open circles indicate the position of Ishigaki Island.

Ishigaki Island, none of the outer rainbands passed over Ishigaki Island.

[18] These meteorological observation results show that our observations at Ishigaki Island captured the front, central, and rear structures of Shanshan.

3.2. Isotopic Characteristics of Precipitation and Water Vapor

[19] From 11 to 18 September 2006, 26 water vapor and 55 precipitation samples were successfully collected. Figure 6 shows the time series of isotope ratios of precipitation and water vapor observed at Ishigaki Island, together with their d-excess values. Although the water vapor sampling was conducted at 6-h intervals, we also irregularly carried out water vapor sampling from 2020–2130 UTC on 15 September during the passage of the eye. Unfortunately, a deficiency of liquid nitrogen due to a power failure interrupted the water vapor sampling from 1630 UTC on 16 September to 0430 UTC on 17 September.

[20] The isotope values of water vapor showed a large range. The isotope ratio gradually decreased from –13 per mil at 2230 UTC on 14 September to –24 per mil at 1630 UTC on 15 September. An anomalously high isotope ratio of –13 per mil appeared at 2100 UTC on 15 September. After 0430 UTC on 16 September, isotope ratios of about –16 per mil for water vapor remained steady. The

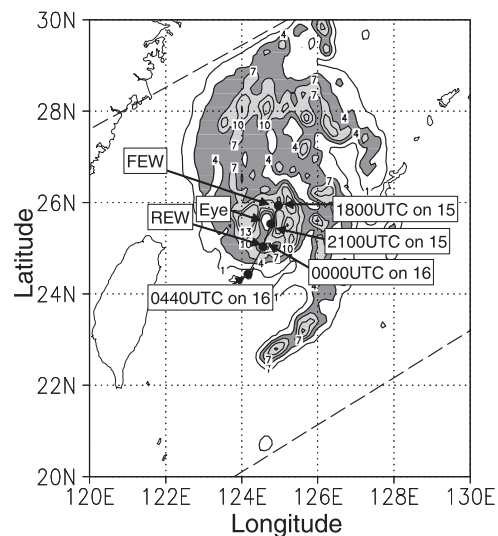


Figure 5. Surface precipitation map derived from TRMM-TMI at 0440 UTC on 16 September 2006. Regions of echo intensity of 4–7 mm are shown by light shading, while regions greater than 7 mm are indicated by heavier shading. The contour interval is 3 mm. A solid line and closed circles represent the position of Ishigaki Island in relation to the TC center.

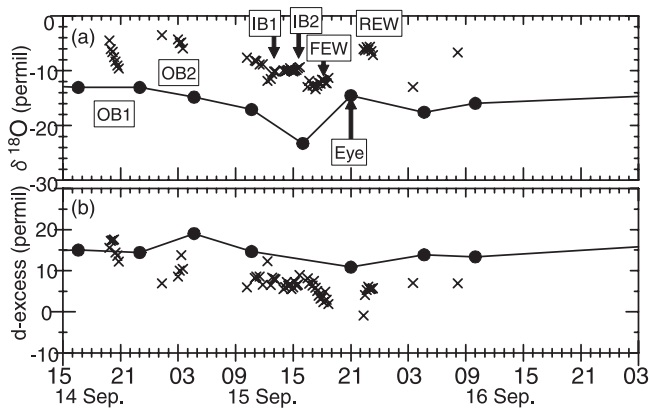


Figure 6. Record of (a) $\delta^{18}\text{O}$ and (b) d-excess of precipitation (crosses) and water vapor (closed circles with solid line) from 1500 UTC on 14 September to 0300 UTC on 17 September 2006. These isotope ratios of precipitation were corrected for sea-spray content.

d-excess of water vapor gradually decreased with a minimum of about 11 per mil at 2100 UTC on 15 September.

[21] The isotopic values of precipitation, which were corrected for sea-spray content, also had a large range. In OB1 and OB2, the isotope ratios of precipitation quickly decreased with significant amplitude by more than 5 per mil. From 1000 UTC on 15 September during the passage of the rain shield over Ishigaki Island, precipitation isotope ratios gradually decreased from -7 to -13 per mil. Abrupt changes in the precipitation isotope ratios occurred at 1230 and 1530 UTC around the passage of IB1 and IB2. The precipitation isotope ratios slightly increased around 1200 and 1800 UTC. Unfortunately, the precipitation samples in the FEW from 1900 to 2100 UTC were not collected. It is remarkable that anomalously high precipitation isotope ratios occurred in the REW around 2200 UTC on 15 September; $\delta^{18}\text{O}$ values of about -6 per mil were as high as those of OB1 and OB2. After the passage of the REW, the isotope ratios in the little precipitation that occurred decreased to -13 per mil at 0330 UTC and increased to -7 per mil at 0800 UTC on 16 September. The d-excess of precipitation of around 10 per mil slightly decreased until

1600 UTC on 15 September, while it quickly decreased from 10 to 0 per mil after 1600 UTC. Figure 7 shows a scatterplot of the $\delta^2\text{H}$ and $\delta^{18}\text{O}$ values of water vapor and precipitation. The samples plotted around the meteoric water line (MWL) [Craig, 1961].

[22] In general, as precipitation continues falling, the isotope ratios of precipitation decrease with increasing precipitation totals, i.e., the so-called amount effect [Dansgaard, 1964]. However, as shown in the isotopic observational results, the variability in the isotope ratios of the precipitation accompanying Shanshan cannot be convincingly explained by the amount effect.

4. Discussion

[23] The isotopic ratios of precipitation and water vapor in Shanshan exhibited systematic variation with the radial distance from the TC center. Figure 8 shows the radial profile of $\delta^{18}\text{O}$ and d-excess of precipitation and water vapor observed at Ishigaki Island. The situation in which the observation site was located on the northern (southern) side of Shanshan and Shanshan approached (moved away from) Ishigaki Island is referred to as the front (rear) side of Shanshan, hereafter.

[24] Between 80 and 300 km radius from the position of OB2 to IB2 in the front side (referred to as the TC's outer region), a clear inward decrease in the isotope ratios of water vapor appeared. The gradient, which is defined as the change in the isotope ratios to the radial distance, was largest in the area outer part of the rain shield in the front side, between 80 and 160 km in radius. In contrast, an inward increase in isotope ratios of water vapor was significant around the eye and eye wall (referred to as the TC's inner region). On the other hand, precipitation isotope ratios gradually decreased inward in the TC's outer region. In the TC's inner region, anomalously high isotope ratios of precipitation appeared in the REW.

[25] We speculate that the observed isotopic variation can primarily be attributed to moisture cycling in the boundary layer. TC-relative winds are divided into two components depending on the wind direction: the tangential wind that flows parallel to curved isobars with velocity defined as positive counterclockwise, and the radial wind that flows toward its center across the isobars with velocity defined as

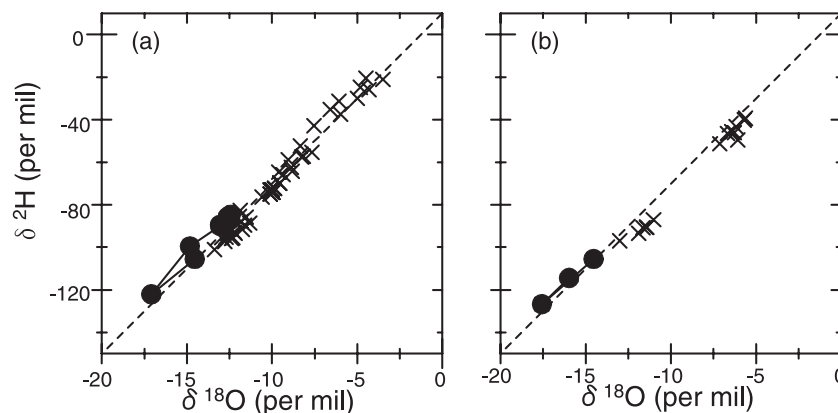


Figure 7. Scatterplot showing $\delta^2\text{H}$ and $\delta^{18}\text{O}$ for precipitation (crosses) and water vapor (closed circles with line) at the (a) front and (b) rear sides of the TC. The broken lines denote the meteoric water line.

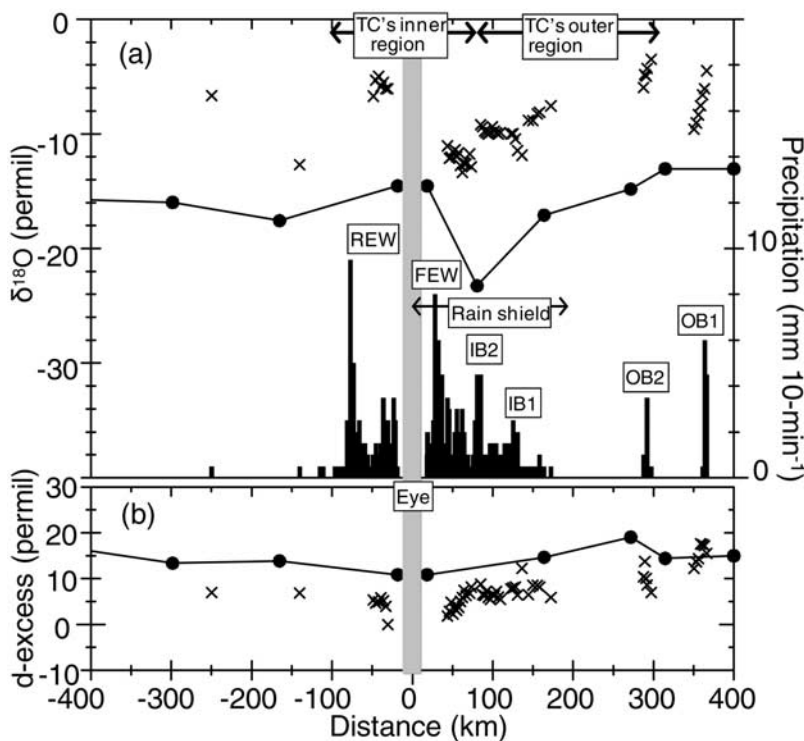


Figure 8. Radial profile of (a) 10-min precipitation (filled bar), $\delta^{18}\text{O}$ and (b) d-excess of precipitation (crosses) and water vapor (closed circles with line). Positive (negative) distance shows the conditions on the front (rear) side of the moving TC. The shaded region in the middle indicates the region of no observations.

positive inward. These winds were derived from the 30-min averaged surface wind observed at JIRCAS, although the wind was not recorded after 1900 UTC on 15 September. Figure 9 shows the radial profile of two wind components. The radial wind increased inward in the TC's outer region. In the TC's inner region, the radial wind decreased inward, while the tangential wind quickly increased inward. This suggests that inward flow was conspicuous in the TC's outer region, whereas relatively weak inward flow and high winds occurred in the TC's inner region.

[26] Isotopic observational results clearly show that the inward decreases in the isotope ratios of water vapor and precipitation appeared in the TC's outer region, where inward flow was conspicuous. The largest gradient was in the precipitation region of the rain shield when the water vapor passed through regions of precipitation. The inward decrease in isotope ratios of water vapor in the TC's outer region was mainly caused by the rainout effect which involves both condensation efficiency as reflected in inwardly increasing cloud thickness and isotopic exchange between falling droplets and ambient water vapor. In active rainout effect, as air masses move through a precipitation region, heavier isotopes are progressively depleted as the air masses lose moisture (e.g., the "continent effect") [Dansgaard, 1964]. In this case, the water vapor was isotopically depleted through the organized precipitation region of Shanshan. Water vapor content would not have decreased due to the radial inward convergence [e.g., Kurihara, 1975]. The precipitation in the TC's outer region was isotopically depleted stepwise by the inward decreases in the isotope ratios of water vapor.

[27] On the other hand, anomalously high isotope ratios of water vapor occurred in the TC's inner region where inward flow was relatively weak and surface wind velocity was high. Figure 2e shows the salinity in collected precipitation samples. The salinity was anomalously high around the TC center, indicating that sea spray filled the atmosphere due to the high winds over the sea surface. Under high winds and the resulting extensive formation of sea spray, the surface area of liquid water of sea spray and sea surface exposed to water vapor increases tremendously. Sea spray, which has heavy isotope ratios like those of ocean water, underwent diffusive isotopic exchange with water vapor before falling back to the sea surface, resulting in the offset the radially inward decrease of isotope ratios. Also the evaporation from the sea surface caused the heavy isotope ratios in water vapor. We refer to these effects as "isorecharge". Because of limitations of the observational data, quantitative understanding of the two kinds of isorecharge remains unclear. However, in the TC's inner region, weak inward flow weakened the rainout effect and the impact of the isorecharge became significant, causing the anomalously high isotope ratios of the water vapor. The precipitation in the eye wall was also isotopically enriched by the water vapor with heavy isotope ratios.

[28] Another remarkable change in the isotopic composition during the passage of Shanshan was the decrease in the d-excess of both precipitation and water vapor in the TC's inner region. The physical processes that affect d-excess are evaporation and diffusive water vapor change in subsaturated air, while the production of precipitation from water vapor essentially conserves the d-excess. The d-excess

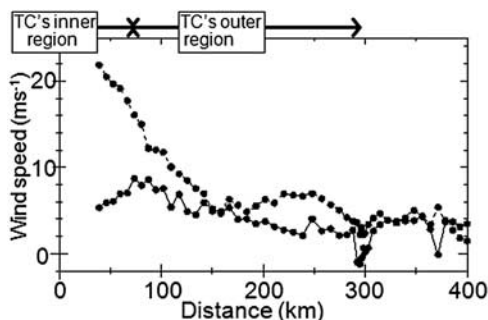


Figure 9. Radial profile of radial (solid line) and tangential (broken line) winds derived from 30-min averaged surface winds observed at Ishigaki Island.

of evaporated vapor from the water surface decreases (increases) as the relative humidity of surface air increases (decreases) [Craig and Gordon, 1965]. Moreover the d-excess of water vapor that undergoes diffusive isotopic exchange with sea spray decreases. Therefore the lower d-excess of water vapor in the TC's inner region can be attributed to the intensive isotopic exchange between water vapor and liquid water, given the TC's high relative humidity of more than 90% (Figure 2c). A unique circumstance of a TC is the intensity of isotopic exchange between water vapor and liquid water of sea spray and sea surface with almost saturated surface air and high winds, leading to anomalously high isotope ratios and low d-excess values of water vapor in the TC's inner region.

[29] Interestingly, there were short-term variations in precipitation isotope ratios within individual rainbands. Precipitation isotope ratios accompanying the outer rainbands OB1 and OB2 spatially decreased with significant amplitude (Figure 8). In the front side of the TC, outer rainbands quickly moved, causing convective precipitation with subsequent stratiform precipitation over Ishigaki Island. Since condensation in the convective region reduces the isotope ratio of the water vapor in saturated rising air by removing the heavy isotopes as precipitation [e.g., Gedzelman and Lawrence, 1990; Gedzelman and Arnold, 1994], the isotope ratios of remaining water vapor in the subsequent stratiform region become lighter, causing precipitation isotope ratios to decrease both downwind and with time (Figures 6 and 8), one of the rainout effects [Gedzelman and Lawrence, 1982]. On the other hand, during the passage of the inner rainbands IB1 and IB2, short-term changes in precipitation isotope ratios had high variability. A short-term isotopic variability in the rain shield is expected depending on the trajectory taken by each air parcel as it travels through regions of convective and stratiform precipitation. Detailed trajectories are needed and this may not be possible without suitable meteorological data and numerical simulation data to obtain the trajectories. Such complex moisture cycling in the multiple clouds of TCs should be considered in future studies.

5. Summary

[30] Isotope ratios of precipitation and water vapor during the passage of Typhoon Shanshan were observed at Ishigaki

Island, Japan. Isotopic observations at observational intervals of 6 h for water vapor sampling and 1-mm amounts of precipitation for precipitation sampling allow for a better qualitative understanding of the atmospheric moisture cycling of TCs. Observational results are summarized as follows: the isotope ratios of both precipitation and water vapor decreased radially inward in the TC's outer region; anomalously high isotope ratios of both precipitation and water vapor appeared in the TC's inner region; and the d-excess of both precipitation and water vapor tended to decrease in the TC's inner region.

[31] Figure 10 illustrates the moisture cycling in a developing TC that controls the observed isotopic features with the radial distance from the TC center. In the TC's outer region, where inward flow was conspicuous in the boundary layer, the water vapor was isotopically depleted due to the rainout effect which involves both condensation efficiency as reflected in inwardly increasing cloud thickness and isotopic exchange between falling droplets and the ambient water vapor. In the TC's inner region, where inward flow was relatively weak and surface wind velocity was high, water vapor was isotopically enriched by weak rainout effect and intensive isorecharge from sea spray and sea surface with heavy isotope ratios. Since water vapor mainly acts as a source of precipitation, the isotope ratios of precipitation also had systematic variation. A unique circumstance of a TC is the intensity of isotopic exchange between water vapor and liquid water of sea spray and sea surface with almost saturated surface air and high winds, leading to anomalously high isotope ratios and low d-excess values in the TC's inner region.

[32] These isotopic observational findings indicate a significant possibility of differences in moisture cycling between the inner and outer regions of a TC developing over the sea, although we still need to verify the possibility quantitatively by using numerical models on the water budget in a TC [e.g., Braun, 2006], for example. Future work will involve the development of a mesoscale isotopic model to realistically simulate the isotopic features observed in Shanshan and quantitatively discuss the moisture cycling related to the intensification of TCs over the sea.

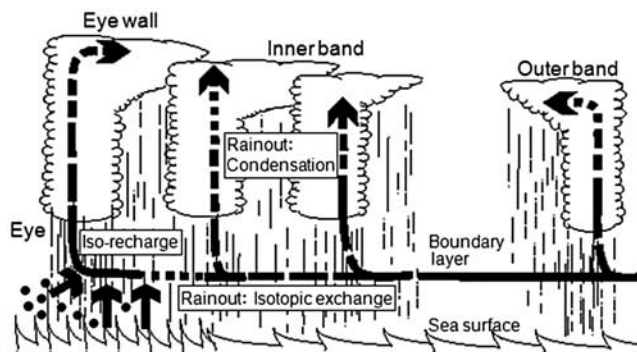


Figure 10. Schematic cross section of moisture cycling in a developing TC. Solid arrows indicate trajectories of isotopically heavier water vapor, while open arrows indicate trajectories of isotopically lower water vapor. Filled circles represent sea spray.

[33] **Acknowledgments.** We are grateful for the assistance of many scientists at the Japan International Research Center for Agricultural Sciences. Thanks are also extended to the Japan Meteorological Agency for supplying meteorological data on Typhoon Shanshan. This work was supported by a Grant in Aid for Young Scientists, (B) 18740302, from the Ministry of Education, Sports, Culture, Science, and Technology, Japan. Additional support has been provided by the Institute of Observational Research for Global Change, Japan Agency for Marine-Earth Science and Technology.

References

- Black, P. G., R. W. Burpee, N. M. Dorst, and W. L. Adams (1986), Appearance of the sea surface in tropical cyclones, *Weather Forecast.*, *1*, 102–107.
- Braun, S. A. (2006), High-resolution simulation of hurricane Bonnie [1998]. Part II: Water budget, *J. Atmos. Sci.*, *63*, 43–64.
- Charney, J. G., and A. Eliassen (1964), On the growth of the hurricane depression, *J. Atmos. Sci.*, *21*, 68–75.
- Craig, H. (1961), Isotopic variations in meteoric waters, *Science*, *133*, 1702–1703.
- Craig, H., and L. I. Gordon (1965), *Stable Isotopes in Oceanic Studies and Paleotemperatures*, 122 pp., V. Liscchi e Figli, Pisa.
- Dansgaard, W. (1964), Stable isotopes in precipitation, *Tellus, Ser. A and Ser. B*, *16*, 436–468.
- Ehhalt, D. H., and H. G. Ostlund (1970), Deuterium in Hurricane Faith, 1966: Preliminary results, *J. Geophys. Res.*, *75*, 2323–2327.
- Emanuel, K. A. (1989), The finite-amplitude nature of tropical cyclogenesis, *J. Atmos. Sci.*, *46*, 3431–3456.
- Gedzelman, S. D., and R. Arnold (1994), Modeling the isotopic composition of precipitation, *J. Geophys. Res.*, *99*, 10,455–10,571.
- Gedzelman, S. D., and J. R. Lawrence (1982), The isotopic composition of cyclonic precipitation, *J. Appl. Meteorol.*, *21*, 1385–1404.
- Gedzelman, S. D., and J. R. Lawrence (1990), The isotopic composition of precipitation from two extratropical cyclones, *Mon. Weather Rev.*, *118*, 495–509.
- Gedzelman, S. D., J. R. Lawrence, J. Gamache, M. Black, E. Hindman, R. Black, J. Dunion, H. Willoughby, and X. Zhang (2003), Probing hurricanes with stable isotopes of rain and water vapor, *Mon. Weather Rev.*, *131*, 1111–1127.
- Ichiyangi, K., K. Yoshimura, and M. D. Yamanaka (2005), Validation of changing water origins over Indochina during the withdrawal of the Asian monsoon using stable isotopes, *SOLA*, *1*, 113–116.
- Kurihara, Y. (1975), Budget analysis of a tropical cyclone simulated in an axisymmetric numerical model, *J. Atmos. Sci.*, *32*, 25–59.
- Lawrence, J. R. (1998), Isotope spikes from tropical cyclones in surface waters: Opportunities in hydrology and paleoclimatology, *Chem. Geol.*, *144*, 153–160.
- Lawrence, J. R., and S. D. Gedzelman (1996), Low stable isotope ratios of tropical cyclone rains, *Geophys. Res. Lett.*, *23*, 527–530.
- Lawrence, J. R., and S. D. Gedzelman (2003), Tropical ice core isotopes: Do they reflect changes in storm activity?, *Geophys. Res. Lett.*, *30*(2), 1072, doi:10.1029/2002GL015906.
- Lawrence, J. R., S. D. Gedzelman, X. Zhang, and R. Arnold (1998), Stable isotopes of rain and vapor in 1995 hurricanes, *J. Geophys. Res.*, *103*, 11,381–11,400.
- Lawrence, J. R., S. D. Gedzelman, M. Black, and J. Gamache (2002), Stable isotopes of precipitation collected at 3 km elevation in Hurricane Oliva [1994], *J. Atmos. Chem.*, *41*, 67–82.
- Lawrence, J. R., S. D. Gedzelman, D. Dexheimer, H. Cho, G. D. Carrie, R. Gasparini, C. R. Anderson, K. P. Bowman, and M. I. Biggerstaff (2004), Stable isotopes composition of water vapor in the tropics, *J. Geophys. Res.*, *109*, D06115, doi:10.1029/2003JD004046.
- Lawrence, J. R., S. Sarnuebti, S. D. Gedzelman, and Kwab-yin Kong (2006), Stable isotope ratios of rain and water vapor in Hurricanes Ivan [2004] and Katrina [2005], in *Preprints AMS Meeting: 27th Conference on Hurricanes and Tropical Meteorology*, Monterey, 24–28 April 2006, Abstract 7B.4.
- Merlivat, L., and Z. Jouzel (1979), Global climatic interpretation of the deuterium oxygen 18 relationship for precipitation, *J. Geophys. Res.*, *84*, 5029–5033.
- Miyake, Y., O. Matsubaya, and O. Nishihara (1968), An isotopic study of meteoric precipitation, *Pap. Meteorol. Geophys.*, *19*, 243–266.
- Montgomery, M. T., M. E. Nicholls, T. A. Cram, and A. B. Saunders (2006), A vertical hot tower route to tropical cyclogenesis, *J. Atmos. Sci.*, *63*, 355–386.
- Ooyama, K. (1964), A dynamical model for the study of tropical cyclone development, *Geofis. Int.*, *4*, 187–198.
- Ooyama, K. V. (1969), Numerical simulation of the life cycle of tropical cyclones, *J. Atmos. Sci.*, *26*, 3–40.
- Rotunno, F., and K. Emanuel (1987), An air-sea interaction theory for tropical cyclones. Part II: Evolutionary study using a nonhydrostatic axisymmetric numerical model, *J. Atmos. Sci.*, *44*, 542–561.
- Shimazu, Y. (1998), Classification of precipitation systems in mature and early weakening stage of typhoon around Japan, *J. Meteorol. Soc. Jpn.*, *76*, 437–445.
- Sugimoto, A., N. Yanagisawa, D. Naito, N. Fujita, and C. Maximov (2002), Importance of permafrost as a source of water for plants in East Siberian Taiga, *Ecol. Res.*, *17*, 493–503.
- Wang, Y., J. D. Kepert, and G. Holland (2001), On the effect of sea spray evaporation on tropical cyclone boundary layer structure and intensity, *Mon. Weather Rev.*, *129*, 2481–2500.

H. Fudeyasu, K. Ichiyangi, and M. D. Yamanaka, Institute of Observational Research for Global Change, Japan Agency for Marine-Earth Science and Technology, 2-15 Natsushima, Yokosuka, Kanagawa, 237-0061, Japan. (fudeyasuh@jamstec.go.jp; kimpei@jamstec.go.jp; mdy@jamstec.go.jp)

K. Ozawa, Japan International Research Center for Agricultural Sciences, 1091-1, Maezato-Kawarabaru, Ishigaki, Okinawa 907-0002, Japan. (kozawa@affrc.go.jp)

A. Sugimoto and A. Ueta, Graduate School of Environmental Science, Hokkaido University, 10-5 Kita, Kitaku, Sapporo, Hokkaido 020-0810, Japan. (sugimoto@star.dti2.ne.jp; a-ueta@ees.hokudai.ac.jp)

K. Yoshimura, Institute of Industrial Science, University of Tokyo, 4-6-1 Komaba, Meguro-ku, Tokyo 153-8505, Japan. (kei@iis.u-tokyo.ac.jp)